Cerebral Perfusion Imaging by Bolus Tracking

Leif Østergaard, MD, MSc, PhD

Summary: Cerebral perfusion may be visualized by the dynamic imaging of an intravenously injected bolus (a few milliliters) of clinically approved gadolinium-containing contrast media. During its passage through the vasculature of the brain, the contrast agent induces magnetic field disturbances, which can be seen as signal loss on appropriately weighted dynamic MRI. This article deals with the quantitative analysis of such signal changes, first in terms of tracer concentration and then, via the mathematical approach of deconvolution, in terms of tissue microvascular physiology, culminating in quantitative estimates on a pixel-by-pixel basis of physiologic parameters, such as cerebral blood volume, mean transit time, and cerebral blood flow.

Key Words: bolus tracking, perfusion, CBV, CBF, deconvolution

(*Top Magn Reson Imaging* 2004;15:3–9)

Perfusion measurements by dynamic susceptibility contrast MRI uses very rapid imaging (most commonly echo planar imaging, EPI) to capture the first pass of intravenously injected paramagnetic contrast agent, hence the term "bolus tracking." By kinetic analysis of these data, hemodynamic indices, namely, cerebral blood flow (CBF), cerebral blood volume (CBV), and mean transit time (MTT) can be derived.

In the following sections, the background of bolus tracking is explained in more detail, including sequence considerations and analysis methods.

SUSCEPTIBILITY CONTRAST

Bolus tracking is commonly carried out using dynamic susceptibility contrast imaging, tracking the passage of a rapidly injected bolus of paramagnetic gadolinium (Gd) chelate by a T_2 (SE) or T_2*-weighted (GE) EPI sequence. In the brain, the first pass extraction of contrast agent is zero when the blood–brain barrier is reasonably intact. This intravascular compartmentalization of contrast agent creates large, microscopic susceptibility gradients, and the dephasing of spins as they diffuse among these result in signal loss in T_2- and T_2*-weighted images, as described by Villringer et al. in 1998.[1]

Spin Echo Versus Gradient Echo

Whereas pulse sequences without full refocusing of static field inhomogeneities (GEs) will experience a general signal loss due to the presence of microscopic field perturbers in the vessels, the signal loss is far less for pulse sequences where dephasing is partially refocused (SEs).

For the SE sequence, signal loss is observed at long echo times, during which water diffuses through areas of different magnetic fields. The signal loss is most pronounced when most spins in or near the contrast-filled vessel have the opportunity to diffuse across the susceptibility gradient at the vessel walls in the course of the echo time TE. The diffusion-related signal loss is hence a complex function of TE, the density of distribution of vessel sizes, and the concentration and magnetic properties of the contrast agent.

Weisskoff and co-workers performed a detailed analysis of these effects using Monte Carlo modeling as well as experimental data.[2–4] They found that SE measurements are mainly sensitive to vessel sizes comparable to the water diffusion length during the time of echo (~10 μm), whereas GE measurements are equally sensitive to all vessel sizes. This effect is illustrated in Figure 1. In practice, imaging performed using an SE approach requires twice the amount of contrast agent (usually a double dose of standard Gd chelate, which is equivalent to 0.2 mmol/kg) compared to imaging with GE-EPI (where 0.1 mmol/kg is generally injected). An in vivo example is shown in Figure 2. In return for this, SE theoretically yields higher sensitivity in detecting changes in small vessel density Furthermore, preliminary studies suggest that, in the brain, the microvascular CBV "visible" by SE-EPI is roughly 45% of the "total" CBV compared with measurements using PET[5] or GE-EPI.[6]

THEORY

To derive hemodynamic parameters from dynamic MR images by tracer kinetic analysis, the contrast agent concentrations in various tissue compartments must be known. For a given pulse sequence (eg, SE or GE EPI), the relation between observed signal changes during the contrast agent bolus passage and the corresponding concentration must be known in detail.

From the Department of Neuroradiology, Center for Functionally Integrative Neuroscience, Aarhus University Hospital, Denmark.

Address of correspondence and reprint requests to Leif Østergaard, MD, MSc, PhD, DMSc, Department of Neuroradiology, Centre for Functionally Integrative Neuroscience (CFIN), Building 30, Aarhus University Hospital, Nørrebrogade 44, 8000 Århus C, Denmark (e-mail: leif@pet.auh.dk).

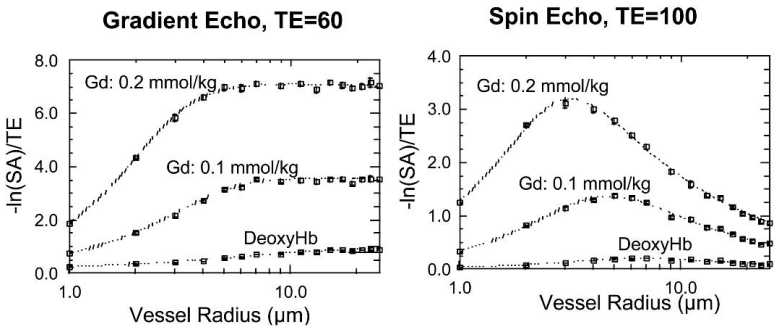

FIGURE 1. The change in transverse relaxation rate as a function of vessel size for typical gadolinium dosages (single and double dose; 0.1 and 0.2 mmol/kg, respectively) and deoxyhemoglobin in SE and GE sequences with typical TE values. Note the microvascular sensitivity of the SE sequence (in the range of capillary diameters), while GE sequences are equally sensitive to all vessel sizes.

An approximate linear relationship exists between tissue contrast agent concentration and change in T_2 / T_2* relaxation rate.

$$\Delta R_2(t) \propto C_t(t) \quad (1)$$

where $R_{2(*)}$ characterizes the relaxation rate change for an SE or GE and $C_t(t)$ refers to the contrast agent concentration of the tissue. This relationship is a central assumption in the subsequent kinetic analysis.

For both GE and SE sequences, signal intensity changes after contrast agent administration, S(t), depend on transverse and longitudinal relaxation rate changes, $\Delta R_{2(*)}$ and ΔR_1, and are described in an exponential fashion as:

$$S(t) = S(t_0)(1 - \exp^{TR\cdot\Delta R_1(t)}) \cdot \exp^{TE\cdot\Delta R_2(t)} \quad (2)$$

where $S(t_0)$ is the baseline signal intensity, TR is the repetition time, and TE is the echo time.

Assuming that R_1 remains constant and is very small (in the brain T1 effects are small because only a small fraction of the tissue water can sample the contrast agent, which is restricted within a small vascular volume assuming blood–brain barrier integrity), Eq. 1 and Eq. 2 can be combined and the relation between concentration and signal intensity is as follows:

$$C_t(t) = -k \cdot \log\left(\frac{S(t)}{S(t_0)}\right)/TE \quad (3)$$

where k is a proportionality constant, which depends on the tissue, the contrast agent, the field strength, and the pulse sequence parameters.

The assumption of linearity in Eq. 1 has been confirmed by indirect measurements in vivo[6] and is now widely used for deriving perfusion measurements. $S(t_o)$ is usually determined from the baseline signal in the images prior to the contrast bolus arrival.

However, in a simulation study performed by Kiselev and Posse, it was found that due to the complex physics of MR signal formation in perfused tissues,[7,8] the linearity in Eq. 3 may not hold for all ranges of contrast agent concentrations or tissues and may cause overestimation of perfusion estimates.[9]

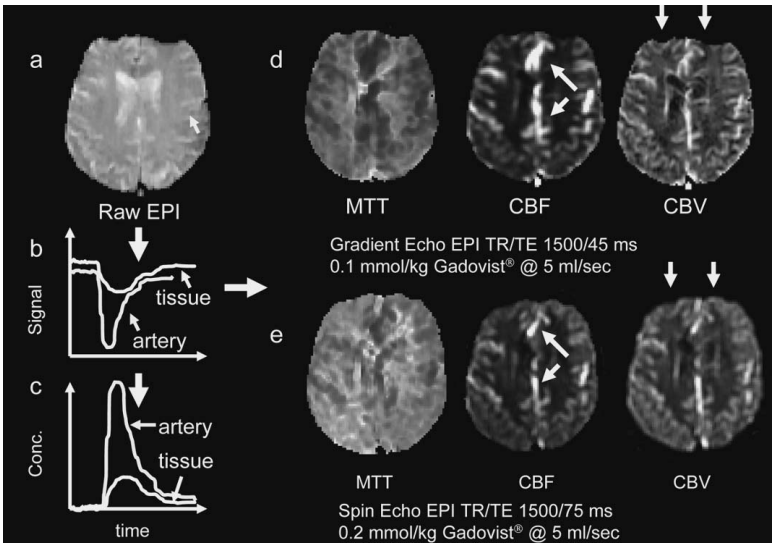

FIGURE 2. The time course of a typical dynamic susceptibility contrast imaging experiment. Upon injection of contrast agent into an antecubital vein, the contrast agent reaches the brain, causing a substantial signal drop in tissue and arteries (**b**), which in turn is converted into contrast agent concentration (**c**). Based on the raw images (**a**), maps of CBF, CBV, and MTT can be derived. Note that the GE raw images are more prone to susceptibility artifacts near tissue–air interfaces, eg, near the frontal sinus (a and **d**) than SE images (**e**). Microvascular sensitivity of the SE sequence makes large vessels less pronounced in the CBF maps (arrows, d and e). Because of the rapid bolus transit, rapid imaging is required to capture the first pass of the bolus (typically at a rate of 1 image / 1.5 second using FLASH or multislice EPI sequences). Rapid injection of contrast agent and saline (preferably flush with 20 mL in adults) is imperative to obtain a sharp input bolus to the tissue.

CBV MEASUREMENTS

Rosen et al. derived maps of relative CBV by kinetic analysis of the concentration time curves while dynamically tracking the bolus passage of a high-susceptibility contrast agent.[10–13] Note that the technique is applicable to any passage tracking of intravascular tracers with high temporal resolution, irrespective of modality (dynamic CT is also suited for this purpose).

The key issue is temporal resolution of the dynamic imaging relative to the characteristic blood transit time of the tissue (typically 4–6 seconds). With a standard 5-mL/second injection into an antecubital vein, the tissue bolus passage duration is of the order of 12 to 20 seconds in adults. With echo planar imaging, a typical choice of temporal resolution is a TR of 1.5 seconds or faster. With current high performance gradient systems, this allows acquisition of 10 to 15 slices (typically with a spatial resolution of roughly 1.5 mm in-plane, 5–6 mm slice thickness) for every TR, providing good brain coverage. For purposes involving deconvolution processes, temporal resolution slower than 1.5 second per image is not advised.

By detecting the arterial as well as the total tissue concentration as a function of time during a single transit, CBV can be determined from the ratio of the areas under the tissue and arterial concentration time curves[14–17]:

$$CBV = \frac{\int_{-\infty}^{\infty} C_t(\tau)d\tau}{\int_{-\infty}^{\infty} C_a(\tau)d\tau} \quad (4)$$

where $C_t(\tau)$ is tissue contrast agent concentration and $C_a(\tau)$ is the arterial contrast agent concentration. These can be determined from Eq. 3.

As arterial measurements (due to limited spatial resolution) are not readily quantifiable, relative CBV values are usually reported. Assuming uniform arterial concentration profiles in all arterial inputs, relative CBV measurements are determined by simply integrating the area under the concentration time curve,[10–12] or occasionally by the use of a gamma variate function in order to correct for tracer recirculation.[18] In a recent report, Perkiö et al.[19] concluded that for relative CBV measurements, typical for clinical assessment of focal pathologies, numerical integration over the whole image range is optimal in terms of computation efficiency, signal-to-noise ratio and accuracy of relative values. However, for absolute CBV measurements, the CBV obtained as the area under the singular value decomposition (SVD) deconvolved tissue curve provides the most accurate estimates.

CBF MEASUREMENTS

The analysis of residue data (ie, the tracer concentration in tissue after a venous injection has reached the tissue through the feeding artery) is most easily understood by first considering a simple experiment where tracer is injected directly into the feeding artery of a tissue element. To describe the tissue retention of tracer, the so-called residue function R is introduced. It measures the fraction of tracer present in the vasculature at time t after injection. So, if the residue is a decreasing function of time, $R(0) = 1$. If the tracer is not bound to the vessels, $R(\infty) = 0$.

For an infinitely short lasting injection that gives rise to an arterial concentration C_a at time 0, the tissue concentration $C_t(t)$ as a function of time is as follows:

$$C_t(t) = CBF \cdot C_a \cdot R(t)$$

This proportionality with CBF is intuitively clear, as the concentration of contrast agent present in the tissue at a given time is proportional to the amount of blood (with tracer concentration C_a) passing through the tissue element per unit time. $CBF \cdot R(t)$ is called the impulse response, as it is the tissue concentration as a result of the aforementioned "impulse" (infinitely short) input.

In real experiments, the arterial input function $C_a(t)$ is distributed in time and the tissue concentration time curves becomes the convolution (sum of individual, very short arterial "impulses" above) of the impulse response and the shape of the arterial input function, which can be mathematically expressed as follows:

$$C_t(t) = CBF\ C_a(t) \otimes R(t) \quad (5)$$

where $\otimes$ indicates a convolution operation.

In order to derive CBF from this equation, the impulse response has to be determined by a process called deconvolution, ie, essentially fitting $CBF \cdot R(t)$ from the experimental data. As $R(0) = 1$, CBF is determined as the initial height of the impulse response function.

A number of difficulties arise when solving Eq. 5. Because of experimental noise, the deconvolution is said to be ill posed, meaning that wildly different solutions for the impulse response can result in similar fits to the experimental data. Approaches to solve this equation in order to regionally determine CBF can be divided into two main categories: 1) model-dependent techniques, where specific analytical expressions are chosen to describe the shape of R(t); and 2) model-independent approaches, where deconvolution is performed for every image pixel, solving Eq. 5 for $CBF \cdot R(t)$. In addition, there are statistical approaches, such as the maximum likelihood technique. As the approach chosen is important in order to understand some of the shortcomings of deconvolution techniques, each of these methods is shortly reviewed below.

DECONVOLUTION TECHNIQUES

Model-Independent Approach

In this approach, Eq. 5 is solved for $CBF \cdot R(t)$ by standard mathematical deconvolution techniques, typically a transform approach, or by a linear algebraic approach.

In the Fourier Transform (FT) approach, the convolution theorem of the FT is utilized, so that the transform of two convolved function equals the product of their individual transforms. Hence, Eq. 5 can be solved[20,21] as:

$$F\{CBF \cdot R(t) \otimes C_a(t)\} = F\{C_t(t)\} \Rightarrow CBF \cdot R(t) = F^{-1}\left\{\frac{F\{C_t(t)\}}{F\{C_a(t)\}}\right\}$$

where F and F^{-1} denote the discrete and inverse discrete Fourier transform.

In the Linear Algebraic Approach, a matrix equation is used.[22] Assuming that tissue and arterial concentrations are measured at equidistant time points t_1, $t_2 = t_1 + \Delta t$,. . .,t_N, the tissue concentration $C(t_j)$ at time t_j can be reformulated as a matrix equation by noting

$$C_t(t_j) = CBF\int_0^{t_j} C_a(\tau)R(t_j - \tau)d\tau \approx CBF\Delta t\sum_{i=0}^{j} C_a(t_i)R(t_j - t_i)$$

equivalent to

$$\begin{pmatrix} C_t(t_1) \\ C_t(t_2) \\ .. \\ C_t(t_N) \end{pmatrix} = CBF \cdot \Delta t \begin{pmatrix} C_a(t_1) & 0 & .. & 0 \\ C_a(t_2) & C_a(t_1) & .. & 0 \\ .. & .. & .. & .. \\ C_a(t_N) & C_a(t_{N-1}) & .. & C_a(t_1) \end{pmatrix} \cdot \begin{pmatrix} R(t_1) \\ R(t_2) \\ .. \\ R(t_N) \end{pmatrix} \quad (6)$$

This is in fact a standard matrix equation that can, theoretically, be inverted to yield CBF·R(t).

Stable solutions for Eq. 5 and Eq. 6 can only be obtained by applying techniques that suppress experimental noise. For the FT, this is achieved by applying a filter to the higher frequencies in the frequency (transformed) domain, under the assumption that this can be done without losing physiological information. In the case of matrix equations, noise is often suppressed by regularization (forcing the solution to satisfy *a priori*, user-defined conditions, or otherwise be well behaved)[23] or by SVD.[22] Further details on noise suppression by SVD are provided by Liu et al.[24]

The optimal choice of some transform and linear algebraic approaches using Monte Carlo simulations was studied by Østergaard et al.[25] It was found that the FT has an inherent problem to derive "true" CBF due to the discontinuity of the impulse response at t = 0 (FTs are optimal for smooth function). In a subsequent analysis by Alsop et al., the SVD and FT were shown to be equivalent when certain periodicity criteria were met.[26] This may also explain the findings of Smith et al.,[27] who found that SVD and FT yield only similar CBF values when tissue concentration curves were first fitted to a gamma variate function. Further evidence suggests that, in normal volunteers, the FT dependence upon vascular structure does not lead to appreciable differences in relative CBF estimates from those obtained by the SVD approach.[28] The FT approach has the attraction of, at least theoretically, being insensitive to delays between the arterial input function and the tissue, as may be observed in cerebrovascular disease.

Of the linear algebraic approaches, regularization showed an inherent dependency on signal-to-noise ratio (and thereby regional blood volume). Deconvolution by SVD showed, however, a remarkable independence upon vascular structure and CBV, yielding reasonably accurate CBF estimates even at signal-to-noise ratio levels of clinical EPI measurements. The major disadvantage of the original SVD approach is a tendency toward underestimation of flow when tissue tracer arrival is delayed relative to the arterial input function.[25,29,30] This problem can be circumvented by the so-called circular SVD, recently published by Wu et al.[31]

Model-Dependent Approaches

The deconvolution techniques described above make no assumptions regarding the vascular structure. Instead, regional vascular transit-time characteristics can be determined along with tissue flow by studying the residue function. Alternative approaches model tracer transport and retention and must therefore be chosen very carefully so as not to lose generality and thereby bias the resulting flow values. Larson et al. suggested an exponential residue model, assuming that the microvasculature behaves like a single, well-mixed compartment[32]. Although residue functions determined by model-less approaches often appear exponential, assumption of this model tends to bias resulting flow values in cases where the underlying residue function is nonexponential.[25]

Østergaard et al. modified and applied a model of macrovascular transport and microvascular retention to the brain.[33] The model, originally introduced to describe tracer transport and retention in the heart,[34,35] uses vascular transport operators, allowing detailed modeling of delay and dispersion of the arterial input due to the passage through the arterial downstream of the measurement site.

Statistical Approaches

Vonken et al. suggested a statistical approach, optimizing the kernel (residue function in Eq. 5) by a maximum likelihood approach. This has the advantage of allowing for delayed tracer arrival relative to the measured arterial input.[36,37] In another statistical approach, Andersen et al. used a Gaussian process to approximate the convolution kernel.[38] Although overly computationally demanding, this represents a promising approach to study the residue function.

Whereas the model-less approach offers simultaneous determination of flow and vascular residue function, the vascular model approach requires a model of major vessel transport as well as of microvascular retention. Major vessel dispersion and microvascular retention can then to some extent be distinguished, stabilizing CBF estimates. On the other hand, abnormal capillary perfusion patterns (and thereby deviation from the normal flow heterogeneity) are likely to affect flow estimates by this approach.[39,40]

MTT

As pointed out by Weisskoff et al., the differentiation between MTT and the first moment of the tissue concentration time curve is crucial in attempting transit time measurements with intravascular tracers.[40] The calculation of MTT requires knowledge of the transport function or CBF and can be formulated using the central volume theorem,[14] which states that:

$$\mathrm{MTT} = \frac{\mathrm{CBV}}{\mathrm{CBF}} \qquad (7)$$

QUANTIFICATION LIMITATIONS

The formalism above produces absolute values for CBF (mL/100 mL/min) and CBV (mL blood/mL tissue), providing arterial and tissue concentrations are experimentally determined in identical units. This, however, presents a number of practical problems in actual clinical applications. Because of the inherently limited spatial resolution of MRI relative to vessel size, absolute arterial tracer concentration measurements are difficult to obtain from image data.

Several studies have applied FLASH-type imaging sequences, allowing measurements of arterial levels in a separate slice (usually placed through the neck) while using a short echo time, and hence avoiding complete loss of vascular signal during bolus passage.[20,37] Studies based on this method yielded somewhat higher absolute CBF values, possibly due to the choice of deconvolution approach or partial volume and averaging effects. However, in a recent study by Schreiber et al., absolute values in good agreement with accepted flow rates were obtained.[41]

In multislice EPI experiments, a single echo is generally used, optimizing tissue signal loss, thereby often causing complete signal loss at major vessels. Therefore, smaller arterial branches with partial volume effects with surrounding tissue are used; consequently, the shape rather than the absolute amplitude of the AIF is obtained in these experiments. Intersubject comparisons must therefore be performed using internal references (eg, white matter or cerebellum), which are supposed to have little intersubject variability. In an attempt to obtain absolute flow values from EPI experiments, Østergaard et al. assumed proportionality between the area of the AIF and the injected contrast dose using water clearance PET as a calibration method. This approach provided reproducible absolute CBF measurements in animal hypercapnia studies[5] and in humans.[42] This approach may, however, be too crude to allow general use in patients with severe cardiac or cerebrovascular disease.

Delay and Dispersion

Even though a simple delay of tracer arrival can be accounted for by, for example, circular SVD, model-less approaches cannot distinguish tracer dispersion in feeding vessels from the tracer retention in the capillary bed. Therefore, large vessel dispersion will be interpreted as slow flow, although actual tissue flow is normal.[25,29] This more fundamental limitation cannot be circumvented unless a specific model dealing with major vessel dispersion is applied.[33]

Using the superior spatial resolution of the raw perfusion images, Alsop et al. suggested detecting the arterial input function regionally, ie, from arterial branches close to the tissue voxel being analyzed.[43] Although correctly assigning the arterial supply of a voxel to one of several nearby arterial branches may be difficult (eg, in vascular watershed areas and in vascular occlusion or stroke), this may be a promising approach in overcoming this inherent methodological problem.

OTHER HEMODYNAMIC INDICES

The derivation of flow and transit times from bolus tracking experiments requires derivation of arterial input tracer levels. In some cases, this may not be practical, as the inherent complexity of deconvolution approaches may preclude the use of these techniques in some situations. Parameters directly obtainable from the tissue concentration time curves (Fig. 3, left panel) are time-to-peak (time from injection to maximum concentration is reached), arrival time (arrival time of tracer in the pixel), full width at half maximum of the tissue bolus shape, as well as the first moment of the peak.

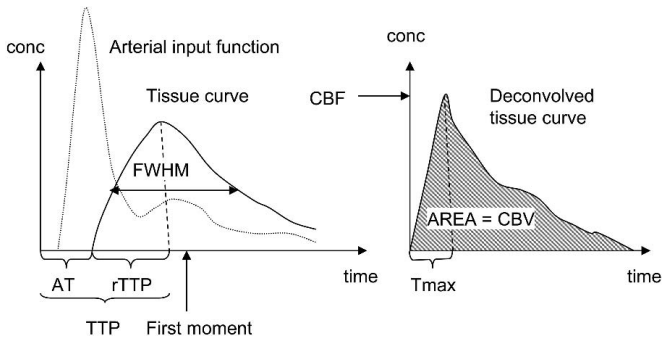

FIGURE 3. Left: Direct descriptors of aspects of the measured concentration-time curves in artery and blood yielding parameters such as "time to peak" and "full width at half maximum." Right: Deconvolution of the arterial curve from the measured tissue curve results in the tissue residue function, whose characteristics can be interpreted as CBF (peak) and CBV (area).

Based on the deconvolved tissue curve (Fig. 3, right panel), a delay of the occurrence of the peak value (the height of the curve, defining CBF) can be defined, which is sometimes referred to as T_{max}.[44]

Although the dependence of these parameters upon MTT and CBF depends strongly on the vascular structure and the arterial input function,[40] they often suffice to delineate pathological changes and can provide important qualitative information in many diseases. However, it appears that the derivation of CBF, CBV, and MTT from kinetic principles improves somehow specificity and sensitivity of clinical studies, facilitating intersubject and intrasubject comparisons.[45]

SUMMARY

In summary, tracking the passage of a contrast agent bolus with fast T_2*-weighted imaging and exploiting the magnetic field disturbance (and T_2*-shortening) associated with the contrast agent allows visualization of cerebral perfusion. Manipulating the signal intensity changes into estimates of tracer (contrast agent) concentration allows tracer kinetic modeling. Absolute concentration determination in arterial structures as well as tissue remains problematic, associated with partial volume effects and differences in agent potency (or relaxivity) as a function of microenvironment. Nonetheless, simultaneous estimation of tracer concentration in a feeding artery and the tissue of interest allows the process of deconvolution to yield quantitative estimates of cerebral blood flow, cerebral blood volume, and mean transit time. These parameters are of considerable clinical impact in the imaging of acute stroke, for example (see also Rowley and Roberts, this issue). A variety of mathematical methods to achieve this deconvolution have been proposed and are under development. Furthermore, the impact of artery choice remains contentious as this may lead to rather different physiologic interpretations. Nonetheless, the methodology presented here demonstrates that magnetic resonance imaging of cerebral perfusion has evolved from a qualitative, to best semiquantitative technique into a more quantitative physiologically specific modality. It is considered likely that this fact will enhance the utility of MR perfusion imaging and identify new roles and applications.

REFERENCES

1. Villringer A, Rosen BR, Belliveau JW, et al. Dynamic imaging with lanthanide chelates in normal brain: contrast due to magnetic susceptibility effects. *Magn Reson Med*. 1988;6:164–174.
2. Fisel CR, Ackerman JL, Buxton RB, et al. MR contrast due to microscopically heterogeneous magnetic susceptibility: numerical simulations and applications to cerebral physiology. *Magn Reson Med*. 1991;17:336–347.
3. Boxerman JL, Hamberg LM, Rosen BR, et al. MR contrast due to intravascular magnetic susceptibility perturbations. *Magn Reson Med*. 1995; 34:555–566.
4. Weisskoff RM, Zuo CS, Boxerman JL, et al. Microscopic susceptibility variation and transverse relaxation: theory and experiment. *Magn Reson Med*. 1994;31:601–610.
5. Østergaard L, Smith DF, Vestergaard-Poulsen P, et al. Absolute cerebral blood flow and blood volume measured by MRI bolus tracking: comparison with PET values. *J Cereb Blood Flow Metab*. 1998;18:425–432.
6. Simonsen CZ, Østergaard L, Vestergaard-Poulsen P, et al. CBF and CBV measurements by USPIO bolus tracking: reproducibility and comparison with Gd-based values. *J Magn Reson Imaging*. 1999;9:342–347.
7. Kiselev VG, Posse S. Analytical theory of susceptibility induced NMR signal dephasing in a cerebrovascular network. *Phys Rev Lett*. 1998;81: 5696–5699.
8. Kiselev VG, Posse S. Analytical model of susceptibility-induced MR signal dephasing: effect of diffusion in a microvascular network. *Magn Reson Med*. 1999;41:499–509.
9. Kiselev VG. On the theoretical basis of perfusion measurements by dynamic susceptibility contrast MRI. *Magn Reson Med*. 2001;46:1113–1122.
10. Rosen BR, Belliveau JW, Vevea JM, et al. Perfusion imaging with NMR contrast agents. *Magn Reson Med*. 1990;14:249–265.
11. Rosen BR, Belliveau JW, Buchbinder BR, et al. Contrast agents and cerebral hemodynamics. *Magn Reson Med*. 1991;19:285–292.
12. Rosen BR, Belliveau JW, Aronen HJ, et al. Susceptibility contrast imaging of cerebral blood volume: human experience. *Magn Reson Med*. 1991; 22:293–299.
13. Belliveau JW. Kennedy-DN, McKinstry RC, et al. Functional mapping of the human visual cortex by magnetic resonance imaging. *Science*. 1991; 254:716–719.
14. Stewart GN. Researches on the circulation time in organs and on the influences which affect it. Parts I-III. *J Physiol (Lond)*. 1894;15:1–89.
15. Meier P, Zierler KL. On the theory of the indicator-dilution method for measurement of blood flow and volume. *J Appl Physiol*. 1954;6:731–744.
16. Zierler KL. Equations for measuring blood flow by external monitoring of radioisotopes. *Circ Res*. 1965;16:309–321.
17. Zierler KL. Theoretical basis of indicator-dilution methods for measuring flow and volume. *Circ Res*. 1962;10:393–407.
18. Thompson HK, Starmer F, Whalen RE, et al. Indicator transit time considered as a gamma variate. *Circ Res*. 1964;14:502–515.
19. Perkiö JP, Aronen HJ, Kangasmaki A, et al. Evaluation of four postprocessing methods for determination of cerebral blood volume and mean transit time by dynamic susceptibility contrast imaging. *Magn Reson Med*. 2002;47:973–981.
20. Rempp KA, Brix G, Wenz F, et al. Quantification of regional cerebral blood flow and volume with dynamic susceptibility contrast-enhanced MR imaging. *Radiology*. 1994;193:637–641.
21. Gobbel GT, Fike JR. A deconvolution method for evaluating indicator-dilution curves. *Phys Med Biol*. 1994;39:1833–1854.
22. Van Huffel S, Vandewalle J, De Roo MC, et al. Reliable and efficient deconvolution technique based on total linear least squares for calculating the renal retention function. *Med Biol Eng Comput*. 1987;25:26–33.
23. Bronikowski TA, Dawson CA, Linehan JH. Model-free deconvolution techniques for estimating vascular transport functions. *Int J Biomed Comput*. 1983;14:411–429.
24. Liu HL, Pu Y, Liu Y, et al. Cerebral blood flow measurement by dynamic contrast MRI using singular value decomposition with an adaptive threshold. Magn Reson Med 1999;167-172.
25. Østergaard L, Weisskoff RM, Chesler DA, et al. High resolution measurement of cerebral blood flow using intravascular tracer bolus passages: I. Mathematical approach and statistical analysis. *Magn Reson Med*. 1996; 36:715–725.
26. Alsop DC, Schlaug G. The Equivalence of SVD and Fourier Deconvolution for dynamic susceptibility contrast analysis. In: *Proc Intl Soc Mag Reson Med.* 2001;9:1581.
27. Smith AM, Grandin CB, Duprez T, et al. Whole brain quantitative CBF and CBV measurements using MRI bolus tracking: comparison of methodologies. *Magn Reson Med*. 2000;43:559–564.
28. Wirestam R, Andersson L, Østergaard L, et al. Assessment of regional cerebral blood flow by dynamic susceptibility contrast MRI using different deconvolution techniques. *Magn Reson Med*. 2000;43:691–700.
29. Calamante F, Gadian DG, Connely A. Delay and dispersion effects in dynamic susceptibility contrast MRI: simulations using singular value decomposition. *Magn Reson Med*. 2000;43:466–473.
30. Wu O, Ostergaard L, Koroshetz WJ, et al. Effects of tracer arrival time on

flow estimates in MR perfusion-weighted imaging. *Magn Reson Med*. 2003;50:856–864.
31. Wu O, Østergaard L, Weisskoff RM, et al. Tracer arrival timing-insensitive technique or estimating flow in MR perfusion-weighted imaging using singular value decomposition with a block-circulant deconvolution matrix. *Magn Reson Med*. 2003;50:100–110.
32. Larson KB, Perman WH, Perlmutter JS, et al. Tracer-kinetic analysis for measuring regional cerebral blood flow by dynamic nuclear magnetic resonance imaging. *J Theor Biol*. 1994;170:1–14.
33. Østergaard L, Chesler DA, Weisskoff RM, et al. Modeling cerebral blood flow and flow heterogeneity from magnetic resonance residue data. *J Cereb Blood Flow Metab*. 1999;19:690–699.
34. King RB, Raymond GM, Bassingthwaighte JB. Modeling blood flow heterogeneity. *Ann Biomed Eng*. 1996;24:352–372.
35. King RB, Deussen A, Raymond GM, et al. A vascular transport operator. *Am J Physiol*. 1993;265:H2196–H2208.
36. Vonken EP, Beekman FJ, Bakker CJ, et al. Maximum likelihood estimation of cerebral blood flow in dynamic susceptibility contrast MRI. *Magn Reson Med*. 1999;41:343–350.
37. Vonken EJPA, van Osch MJP, Bakker CJG, et al. Measurement of cerebral perfusion with dual-echo multi-slice quantitative dynamic susceptibility contrast MRI. *J Magn Reson Imag*. 1999;10:109–117.
38. Andersen IK, Szymkowiak A, Rasmussen CE, et al. Perfusion quantification using Gaussian process deconvolution. *Magn Reson Med*. 2002;48: 351–361.
39. Lassen NA. Cerebral transit of an intravascular tracer may allow measurement of regional blood volume but not regional blood flow [letter]. *J Cereb Blood Flow Metab*. 1984;4:633–634.
40. Weisskoff RM, Chesler D, Boxerman JL, et al. Pitfalls in MR measurement of tissue blood flow with intravascular tracers: which mean transit time? *Magn Reson Med*. 1993;29:553–558.
41. Schreiber WG, Guckel F, Stritzke P, et al. Cerebral blood flow and cerebrovascular reserve capacity: estimation by dynamic magnetic resonance imaging. *J Cereb Blood Flow Metab*. 1998;18:1143–1156.
42. Østergaard L, Johannsen P, Høst-Poulsen P, et al. Cerebral blood flow measurements by MRI bolus tracking: comparison with [^{15}O]H_2O PET in humans. *J Cereb Blood Flow Metab*. 1998;18:935–940.
43. Alsop DC, Wedmid A, Schlaug G. Defining a local input function for perfusion quantification with bolus contrasts MRI. In: *Proc Intl Soc Mag Reson Med.* 2002;10:659.
44. Shih LC, Saver JL, Alger JR, et al. Perfusion-weighted magnetic resonance imaging thresholds identifying core, irreversibly infarcted tissue. *Stroke*. 2003;34:1425–1430.
45. Yamada K, Wu O, Gonzalez RG, et al. Magnetic resonance perfusion-weighted imaging of acute cerebral infarction: effect of the calculation methods and underlying vasculopathy. *Stroke*. 2002;33:87–94.

